Journal of Energy Chemistry 36 (2019) 47–50

Contents lists available at ScienceDirect

Journal of Energy Chemistry

journal homepage: www.elsevier.com/locate/jechem

http://www.journals.elsevier.com/journal-of-energy-chemistry/

Communication

Room-temperature conversion of ethane and the mechanism understanding over single iron atoms confined in graphene

Suheng Wang[a,b,1], Haobo Li[c,1], Mengqi He[d], Xiaoju Cui[a,b], Lei Hua[d], Haiyang Li[d], Jianping Xiao[c], Liang Yu[b], N. Pethan Rajan[b], Zhaoxiong Xie[a], Dehui Deng[a,b,*]

[a] State Key Laboratory for Physical Chemistry of Solid Surfaces, Collaborative Innovation Center of Chemistry for Energy Materials, College of Chemistry and Chemical Engineering, Xiamen University, Xiamen 361005, Fujian, China

[b] State Key Laboratory of Catalysis, Collaborative Innovation Center of Chemistry for Energy Materials, Dalian Institute of Chemical Physics, Chinese Academy of Sciences, Dalian 116023, Liaoning, China

[c] Institute of Natural Sciences, Westlake Institute for Advanced Study, Westlake University, Hangzhou 310024, Zhejiang, China

[d] Key Laboratory of Separation Science for Analytical Chemistry, Dalian Institute of Chemical Physics, Chinese Academy of Sciences, Dalian 116023, Liaoning, China

Dedicated to the 70th anniversary of Dalian Institute of Chemical Physics, CAS, China.

ARTICLE INFO

Article history:
Received 28 February 2019
Revised 2 April 2019
Accepted 3 April 2019
Available online 5 April 2019

Keywords:
Ethane conversion
C–H activation
Graphene
Single iron atom
Room-temperature reaction

ABSTRACT

The catalytic conversion of ethane to high value-added chemicals is significantly important for utilization of hydrocarbon resources. However, it is a great challenge due to the typically required high temperature (> 400 °C) conditions. Herein, a highly active catalytic conversion process of ethane at room temperature (25 °C) is reported on single iron atoms confined in graphene via the porphyrin-like N_4-coordination structures. Combining with the operando time of flight mass spectrometer and density functional theory calculations, the reaction is identified as a radical mechanism, in which the C–H bonds of the same C atom are preferentially and sequentially activated, generating the value-added C_2 chemicals, simultaneously avoiding the over-oxidation of the products to CO_2. The in-situ formed O–FeN_4–O structure at the single iron atom serves as the active center for the reaction and facilitates the formation of ethyl radicals. This work deepens the understanding of alkane C–H activation on the FeN_4 center and provides the reference in development of efficient catalyst for selective oxidation of light alkane.

Dehui Deng's Group for Two-dimensional (2D) Materials & Energy Catalysis. Our research focuses on the development of 2D material-based catalyst and their applications in catalytic conversion of energy molecules, mainly including: (1) Designing and synthesis of advanced 2D materials and their heterostructures, such as graphene, MoS_2, LDHs, for efficient catalytic activities. (2) Thermochemical, electrochemical and thermo-electrical coupled catalysis toward highly efficient activation and conversion of energy molecules, such as O_2, H_2, H_2O, CO, CO_2, CH_4 and CH_3OH. (3) Computational and theoretical modeling of energy catalysis systems to provide fundamental understandings of catalytic activation and reaction mechanism for catalyst optimization and development.

Ethane as one abundant component of natural gas, shale gas and combustible ice, the exploitation has been in rapid growth in recent years [1]. The value-added C_2 chemicals converted from ethane, such as ethanol, acetic acid and ethene, are widely used as fuels, plastic building block, chemical feedstock [2–6], thus the catalytic conversion of ethane is an important process. However, the high bond energy of C–H (409 kJ/mol) makes the process extremely difficult. High temperature (> 400 °C) [7–9] conditions are typically required in the conventional industrial process, which usually brings side-effects such as over-oxidation of the products and carbon deposition on the catalyst.

Recently, it was reported that ethane can be partially oxidized by H_2O_2 in strong acidic medium at 50–180 °C using complexes with metal cores of V, Mn, Fe, Mo, Ru, Pd, Os, and Pt as homogeneous catalysts [10–14]. In addition, the Fe or Cu modified zeolite catalysts exhibited superior performance in ethane partial oxidation at 50 °C using H_2O_2 as oxidant in heterogeneous catalysis

* Corresponding author at: State Key Laboratory of Catalysis, Collaborative Innovation Center of Chemistry for Energy Materials, Dalian Institute of Chemical Physics, Chinese Academy of Sciences, Dalian 116023, Liaoning, China.
E-mail address: dhdeng@dicp.ac.cn (D. Deng).

[1] These authors contributed equally to this work.

https://doi.org/10.1016/j.jechem.2019.04.003

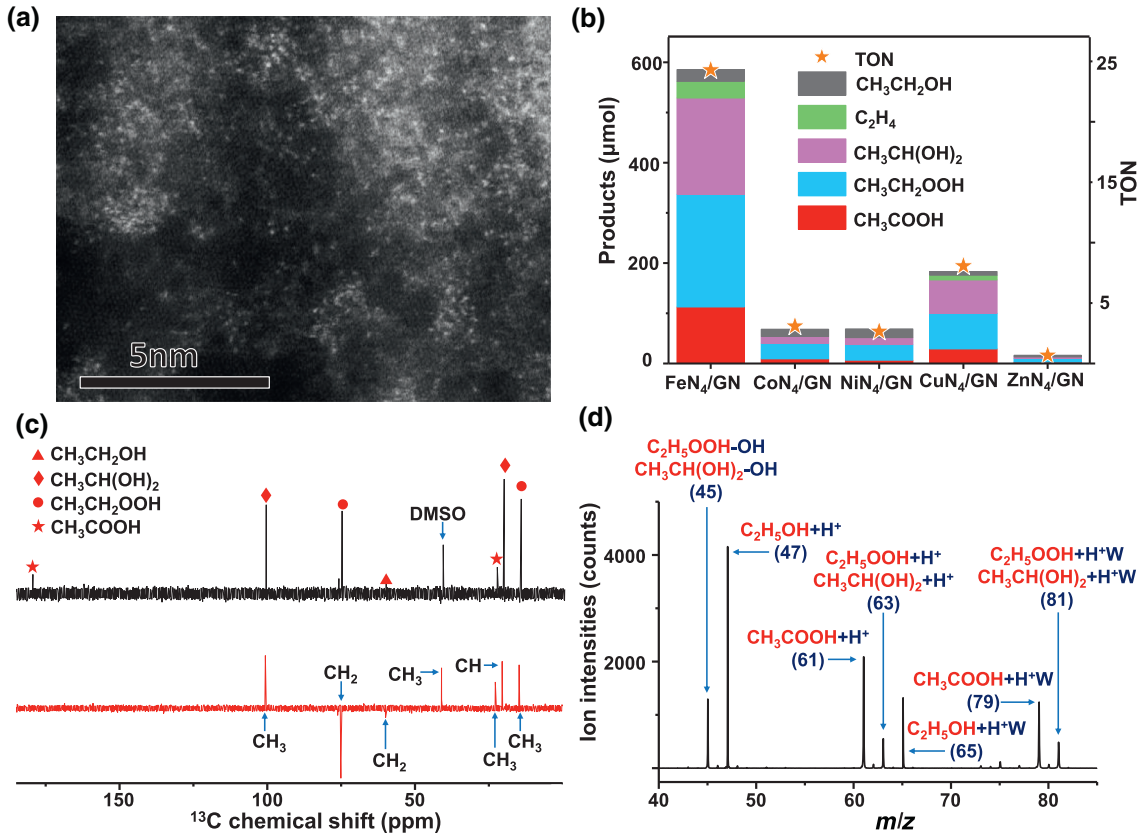

Fig. 1. The structure and catalytic performance of MN_4/GN. (a) HAADF-STEM image of FeN_4/GN. (b) The products of different MN_4/GN (Fe, Co, Ni, Cu, Zn) for ethane oxidation. (c) ^{13}C NMR, ^{13}C DEPT-135 spectra, and (d) TOF-MS spectrum obtained from the reaction of ethane oxidation by FeN_4/GN catalyst. The symbol "W" represents one water molecule. The TOF-MS intensity has been deducted from the background signal that using N_2 as the reaction gas. Reaction conditions in (a–d): 50 mg catalyst, 10 mL H_2O_2 (15%), 1.6 MPa ethane, in a steel autoclave with a Teflon inner vessel (100 mL) at 25 °C for 10 h.

[15–17]. However, achieving ethane conversion at room temperature (25 °C) remains a great challenge.

Herein, we report that single-atom iron with a N_4 coordination [18,19] confined in graphene matrix [20] is highly active for catalytic conversion of ethane to C_2 components (acetic acid (CH_3COOH), ethyl hydroperoxide (CH_3CH_2OOH), 1,1-ethanediol ($CH_3CH(OH)_2$) and ethene (CH_2CH_2)) at room temperature. Besides, the reaction route of ethane oxidation on the catalyst is proposed based on operando time of flight mass spectrometer (TOF-MS), nuclear magnetic resonance (NMR) and density functional theory (DFT) calculations, which indicate that ethane can be easily activated over the in-situ generated O–FeN_4–O active site along a radical mechanism and is finally converted to various value-added products via different free radicals intermediates, such as $\cdot CH_2CH_3$, $\cdot CH(OH)CH_3$ and $\cdot COCH_3$.

A series of 3d transition metal-N_4 (MN_4, M = Fe, Co, Ni, Cu and Zn) centers confined in the matrix of graphene nanosheets (MN_4/GN) were prepared according to our previous reported methods by high-energy ball-milling the mixture of metal phthalocyanines and graphene nanosheets [21–23]. The sub-angstrom resolution high angle annular dark field scanning transmission electron microscopy (HAADF-STEM) image displayed that single iron atoms were distributed homogeneously in graphene nanosheets (Fig. 1a). The structure of FeN_4 was confirmed by extended X-ray absorption fine structure (EXAFS) spectroscopy and low-temperature scanning tunneling microscopy (LT-STM) in our previous work [21].

The ethane oxidation reaction was carried out in an autoclave at room temperature (25 °C) under 1.6 MPa using MN_4/GN as the catalyst and H_2O_2 as the oxidant after the optimization of the H_2O_2 concentration, reaction pressure, and catalyst amount (Figs. S1–S3). The excessive H_2O_2 might break some of FeN_4 active centers, causing the decreasing of conversion (Fig. S1), and therefore a moderate H_2O_2 concentration was used in this study. The reaction products are analyzed by NMR, TOF-MS and gas chromatography (GC). The catalytic activity of various MN_4/GN samples is presented in Fig. 1(b). As shown in Fig. 1(b), FeN_4/GN exhibits the optimum activity for ethane oxidation compared with other metal centers according to the amounts of products and turnover number (TON). The GC characterization results confirm the generation of C_2H_4 in gas phase and the absence of over-oxidized products (CO_2) (Fig. S4). After carefully analyzing the liquid products by various characterization techniques including the ^1H NMR (Fig. S5), ^{13}C DEPT-135 (distortionless enhancement by polarization transfer) (Fig. 1c), ^{13}C NMR (Fig. 1c), and HSQC-NMR (heteronuclear single quantum coherence) (Fig. S6), we found that the ethane can be transformed to C_2 components, i.e. the CH_3CH_2OOH, CH_3COOH, $CH_3CH(OH)_2$ and CH_3CH_2OH at room temperature [15]. Moreover, the structure of these products was also confirmed by the TOF-MS (Fig. 1d). The peaks of CH_3COOH and CH_3CH_2OH can be easily marked. However, the signals of CH_3CH_2OOH and $CH_3CH(OH)_2$ are overlapped due to the same molecular weight. These results are consistent with the NMR data. In addition, considering the catalyst itself contains the carbon sources, we also carried out the contrast test under the N_2 condition (Fig. S7), while the C_2 products were not observed in the ^1H NMR data. It illustrates that the C_2 components come from the ethane rather than the catalyst itself. In addition, the stability tests reveal that the FeN_4/GN can keep the 60% catalytic activity after six cycles, demonstrating its good stability (Fig. S8).

Furthermore, we used the operando TOF-MS to track the reaction process over the FeN_4/GN sample (Fig. S9). The liquid phase

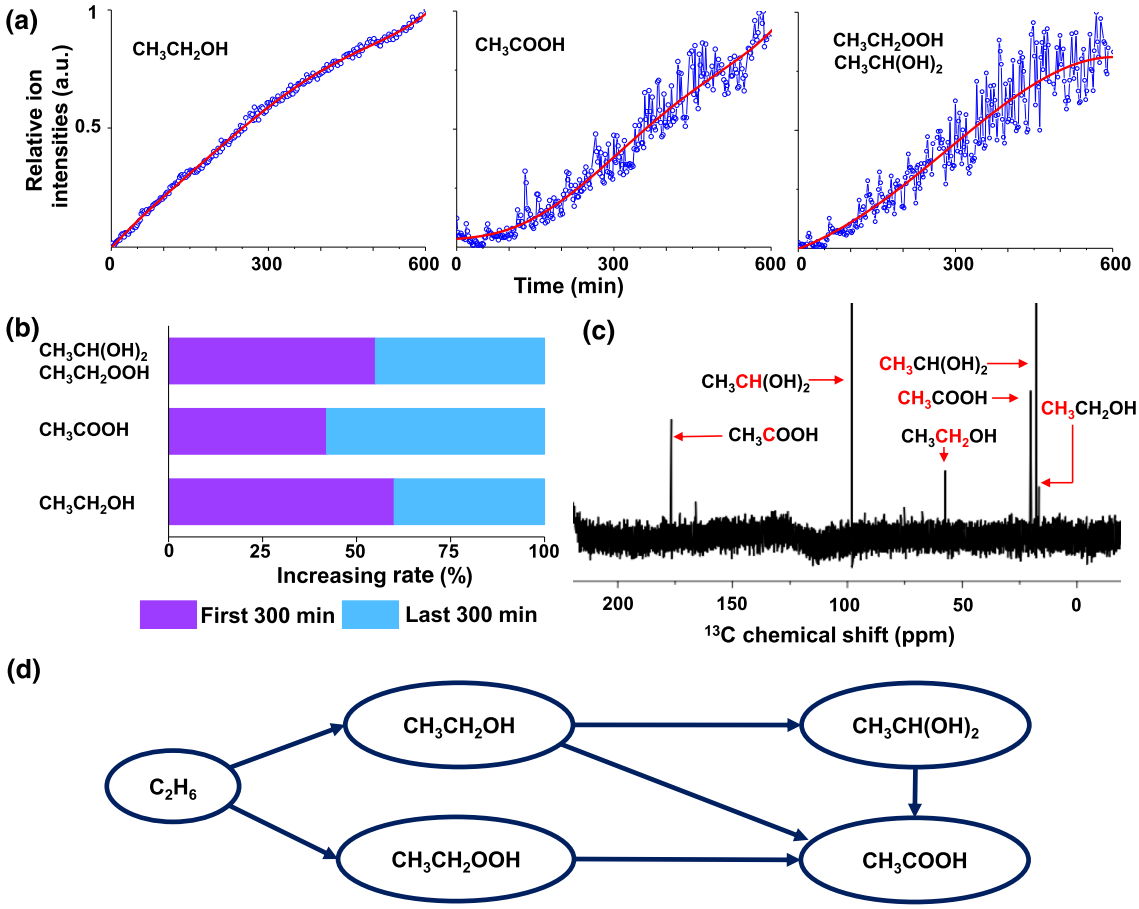

Fig. 2. Mechanism study of FeN_4/GN for ethane conversion. (a) The operando TOF-MS data obtained from C_2H_6 oxidation. (b) The increase rate of the products at 0–600 min, which corresponds to the relative intensity increment. (c) ^{13}C NMR result of CH_3CH_2OH oxidation by FeN_4/GN. (d) A possible reaction path for ethane oxidation over FeN_4/GN catalyst. Reaction conditions in (a): 50 mg catalyst, 10 mL H_2O_2 (15%) at 25 °C for 10 h; in (c): 50 mg catalyst, 10 mL H_2O_2 (15%), 0.05 M CH_3CH_2OH, 1.6 MPa N_2, in a steel autoclave with a Teflon inner vessel (100 mL) at 25 °C for 10 h.

products can be analyzed by TOF-MS in real time through the filter and capillary under the high pressure (typically 1.6 MPa). The increasing rate of different products can be observed during the reaction (Fig. 2a), which were further analyzed towards the increasing rate of the products in the first 300 min and last 300 min (Fig. 2b). The increasing rate of CH_3CH_2OOH, $CH_3CH(OH)_2$ and CH_3CH_2OH in the first 300 min is greater than in the last 300 min. On the other hand, most of CH_3COOH is produced in the last 300 min. Besides, the similar results were also observed under the different pressures (0.8 MPa, 1.2 MPa) in the operando TOF-MS studies (Fig. S10). These results suggest that ethane should be initially converted to CH_3CH_2OH and CH_3CH_2OOH via oxidation of single C–H bond of ethane followed by further oxidation of these products, leading to the formation of CH_3COOH and $CH_3CH(OH)_2$. To confirm this hypothesis, we directly used ethanol as the reactant and obtained the CH_3COOH and $CH_3CH(OH)_2$ (Figs. 2c and S11), which indicates that the ethane can be converted into CH_3COOH and $CH_3CH(OH)_2$ via ethanol. Besides, through controlling the reaction time, it can be observed that the selectivity of CH_3CH_2OOH and CH_3CH_2OH decreases and the selectivity of CH_3COOH and $CH_3CH(OH)_2$ increases during the reaction, which suggests that CH_3COOH and $CH_3CH(OH)_2$ may come from CH_3CH_2OOH and CH_3CH_2OH (Fig. S12). According to the above experimental results, we propose one possible reaction route (Fig. 2d). The ethane is firstly converted to the CH_3CH_2OOH and CH_3CH_2OH. The generated CH_3CH_2OH will be further oxidized to $CH_3CH(OH)_2$ and CH_3COOH. And the CH_3CH_2OOH can also be converted to CH_3COOH.

DFT calculations were carried out to further understand the ethane conversion process. A model of FeN_4 structure confined in the matrix of graphene with the central Fe atom coordinated with four N atoms has been built to simulate the FeN_4/GN catalysts. In the aqueous H_2O_2 environment, FeN_4 is easy to adsorb two O atoms and form the O–FeN_4–O structure (Fig. 3a), which is the active site for C–H bond cleavage [21,23]. The structure of O–FeN_4–O has been proved by X-ray absorption fine structure spectroscopy (XAFS) and Mössbauer spectra in our previous work [21]. The ethane activation is along a radical mechanism. As shown in Fig. S13, the C–H bond of C_2H_6 is stretched on the O–FeN_4–O site, through a transition state (TS) forming a $\cdot CH_2CH_3$ radical, which will bind with the OH group on the surface to generate CH_3CH_2OH, and the left FeN_4–O structure will react with the H_2O_2 in the solution to cycle back to the O–FeN_4–O active structure. The activation barrier is only 0.48 eV, which means the ethane activation can be performed in mild conditions (Fig. 3b). As shown in Fig. 3(a), the $\cdot CH_2CH_3$ radical may also bind with one $\cdot OOH$ group in the H_2O_2 solution to form CH_3CH_2OOH or break another C–H bond to form CH_2CH_2.

The generated CH_3CH_2OH molecules can be further activated on the O–FeN_4–O site. As shown in Figs. S14 and S15, compared with the CH_3 group (barrier: 0.56 eV), the CH_2 group is more easily to be activated (barrier: 0.20 eV) to form $CH_3CH(OH)_2$ radical, which was confirmed by the electron paramagnetic resonance experiments (Figs. S16 and S17). The $CH_3CH(OH)_2$ radical can also be dehydrated to generate CH_3CHO. Moreover, the last C–H bond

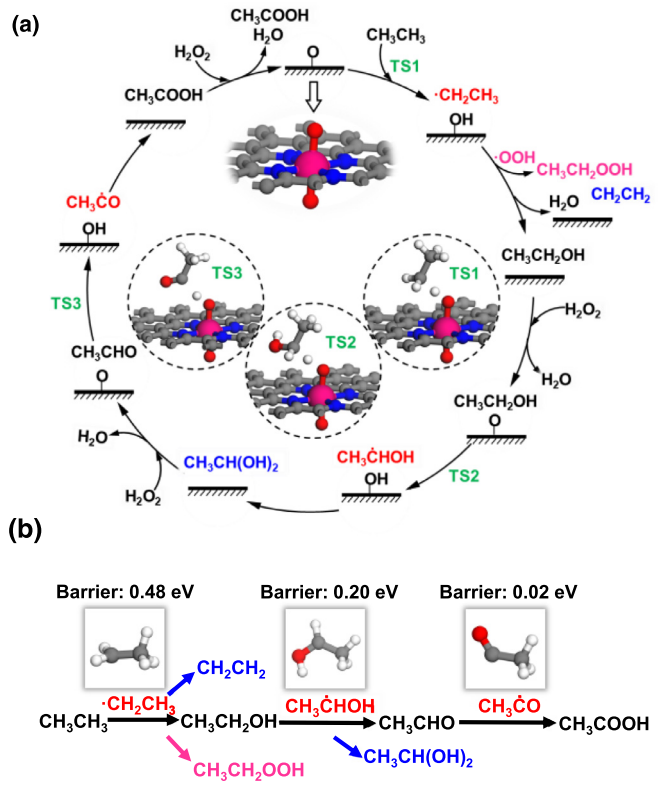

Fig. 3. Proposed mechanism for C_2H_6 activation on the O–FeN_4–O active site. (a) Reaction cycle with the reactants (black), products (black, blue and pink), the radical intermediates (red) and the atomic structures of the active site and transition states TS1–TS3. (b) Reaction pathway with atomic structure of intermediates and the corresponding activation barrier.

on the C atom of CH_3CHO can be very easily activated (barrier: 0.02 eV) to form a further oxidation product CH_3COOH, which explains that almost no aldehyde products were detected. The DFT results agree well with the experimental results.

In conclusion, we report a FeN_4/GN catalyst with high activity for the conversion of ethane to C_2 chemicals at room temperature. Through a series of experiments including operando TOF-MS and DFT calculations, we found that the O–FeN_4–O structure formed in aqueous H_2O_2 is able to convert ethane to ethyl radical in mild conditions. The ethyl radicals will bind with the ·OH and ·OOH groups to form CH_3CH_2OH and CH_3CH_2OOH. Furthermore, through activating the C–H bonds on the same C atom, CH_3CH_2OH could be further converted to $CH_3CH(OH)_2$ and CH_3COOH. These findings provide the reference for understanding and designing highly efficient catalysts for C–H bond activation and conversion.

Acknowledgments

We gratefully acknowledge the financial support from the Ministry of Science and Technology of China (Nos. 2016YFA0204100 and 2016YFA0200200), the National Natural Science Foundation of China (Nos. 21890753, 21573220 and 21802124), the Key Research Program of Frontier Sciences of the Chinese Academy of Sciences (No. QYZDB-SSW-JSC020), and the DNL Cooperation Fund, CAS (No. DNL180201). We also acknowledge the financial and technique supports from the Westlake Education Foundation, Supercomputing Systems in the Information Technology Center of Westlake University.

Supplementary material

Supplementary material associated with this article can be found, in the online version, at doi:10.1016/j.jechem.2019.04.003.

References

[1] R.D. Armstrong, G.J. Hutchings, S.H. Taylor, Catalysts 6 (2016) 71.
[2] L. Kong, J. Li, Q. Liu, Z. Zhao, Q. Sun, J. Liu, Y. Wei, J. Energy Chem. 25 (2016) 577–586.
[3] P. Verma, K.D. Vogiatzis, N. Planas, J. Borycz, D.J. Xiao, J.R. Long, L. Gagliardi, D.G. Truhlar, J. Am. Chem. Soc. 137 (2015) 5770–5781.
[4] B. Liu, S.C. Oh, H. Chen, D. Liu, J. Energy Chem. 30 (2019) 42–48.
[5] H. Zhu, D.C. Rosenfeld, D.H. Anjum, V. Caps, J.M. Basset, ChemSusChem 8 (2015) 1254–1263.
[6] D.J. Xiao, E.D. Bloch, J.A. Mason, W.L. Queen, M.R. Hudson, N. Planas, J. Borycz, A.L. Dzubak, P. Verma, K. Lee, F. Bonino, V. Crocella, J. Yano, S. Bordiga, D.G. Truhlar, L. Gagliardi, C.M. Brown, J.R. Long, Nat. Chem. 6 (2014) 590–595.
[7] M. Peymani, S.M. Alavi, M. Rezaei, Int. J. Hydrogen Energy 41 (2016) 19057–19069.
[8] J. Li, J. Liu, L. Ren, Q. Liu, Z. Zhao, Y. Chen, P. Zhu, Y. Wei, A. Duan, G. Jiang, J. Energy Chem. 23 (2014) 609–616.
[9] X. Li, E. Iglesia, Appl. Catal. A 334 (2008) 339–347.
[10] B.G. Hashiguchi, M.M. Konnick, S.M. Bischof, S.J. Gustafson, D. Devarajan, N. Gunsalus, D.H. Ess, R.A. Periana, Science 343 (2014) 1232–1237.
[11] G.B. Shul'pin, G.V. Nizova, Y.N. Kozlov, L. Gonzalez Cuervo, G. Süss-Fink, Adv. Synth. Catal. 346 (2004) 317–332.
[12] G.B. Shul'pin, G. Süss-Fink, L.S. Shul'pina, J. Mol. Catal. A: Chem. 170 (2001) 17–34.
[13] Q. Yuan, W. Deng, Q. Zhang, Y. Wang, Adv. Synth. Catal. 349 (2007) 1199–1209.
[14] L.S. Shul'pina, M.V. Kirillova, A.J.L. Pombeiro, G.B. Shul'pin, Tetrahedron 65 (2009) 2424–2429.
[15] M.M. Forde, R.D. Armstrong, C. Hammond, Q. He, R.L. Jenkins, S.A. Kondrat, N. Dimitratos, J.A. Lopez-Sanchez, S.H. Taylor, D. Willock, C.J. Kiely, G.J. Hutchings, J. Am. Chem. Soc. 135 (2013) 11087–11099.
[16] Q. Zhang, Y. Wang, Y. Ohishi, T. Shishido, K. Takehira, J. Catal. 202 (2001) 308–318.
[17] R. Armstrong, S. Freakley, M. Forde, V. Peneau, R. Jenkins, S. Taylor, J. Moulijn, D. Morgan, G. Hutchings, J. Catal. 330 (2015) 84–92.
[18] L. Gao, M. Xiao, Z. Jin, C. Liu, J. Zhu, J. Ge, W. Xing, J. Energy Chem. 27 (2018) 1668–1673.
[19] H. Ren, Y. Wang, X. Tang, J. Lu, L. Xiao, L. Zhuang, J. Energy Chem. 26 (2017) 616–621.
[20] H. Xu, L. Ma, Z. Jin, J. Energy Chem. 27 (2018) 146–160.
[21] D. Deng, X. Chen, L. Yu, Q. Liu, Y. Liu, X. Cui, H. Li, J. Xiao, J. Deng, F. Yang, X. Pan, X. Bao, X. Wu, T. Xu, L. Sun, H. Yang, H. Tian, J. Li, Y. Hu, J. Zhou, P. Du, R. Si, J. Wang, P.N. Duchesne, P. Zhang, Sci. Adv. 1 (2015) e1500462.
[22] X. Cui, J. Xiao, Y. Wu, P. Du, R. Si, H. Yang, H. Tian, J. Li, W.H. Zhang, D. Deng, X. Bao, Angew. Chem. Int. Ed. 55 (2016) 6708–6712.
[23] X. Cui, H. Li, Y. Wang, Y. Hu, L. Hua, H. Li, X. Han, Q. Liu, F. Yang, L. He, X. Chen, Q. Li, J. Xiao, D. Deng, X. Bao, Chem 4 (2018) 1902–1910.